Atmospheric Research 268 (2022) 106025

Contents lists available at ScienceDirect

Atmospheric Research

journal homepage: www.elsevier.com/locate/atmosres

Lightning Potential Index and its spatial and temporal characteristics in COSMO NWP model

Iva Babuňková Uhlířová [a,b], Jana Popová [a,b], Zbyněk Sokol [a,*]

[a] Institute of Atmospheric Physics of the Czech Academy of Sciences, Boční II 1401, 141 00 Prague, Czech Republic
[b] Faculty of Science, Charles University, Albertov 6, 128 00 Prague, Czech Republic

ARTICLE INFO

Keywords:
Lightning potential Index
COSMO
Cloud microphysics
Lightning

ABSTRACT

Among severe meteorological hazards, lightning is considered one of the most dangerous; however, its forecast is difficult because the formation of lightning is the result of processes in the clouds that are difficult to model accurately. In this study, we predict lightning activity using the Lightning Potential Index (LPI), which is quite often used to determine areas with expected lightning activity, and analyse its spatial and temporal characteristics. Specifically, we performed simulations of LPI (15 min values) using the COSMO NWP model for 10 selected thunderstorm events of 2018 in Central Europe. We used the model runs with 1- and 2-moment cloud microphysics and with a lead time of 12 h presented in our previous study, while in this study we performed deeper analyses and verified the 15 min LPI values in space and time using ground-based observations of lightning. Our results showed that 2-moment cloud microphysics provide better LPI forecasts which confirms the suggestion of our previous study. The distribution of predicted lightning activity related to the model orography was examined and found consistent with the occurrence of recorded lightning discharges. The Fraction Skill Score analysis revealed that for 2-moment cloud microphysics a skilful forecast was reached at smaller scales than for 1-moment microphysics, namely at scales around 90 km for LPI thresholds 30, 40 and 50 Jkg^{-1}. We also evaluated the forecasts using a performance diagram, which in contrast to other results did not confirm that forecasts using 2-moment cloud microphysical scheme were more accurate than forecasts using 1-moment cloud microphysical scheme. Spatial verification of LPI showed that depending on the distance limit (15–90 km) and the LPI threshold (from LPI > 0 Jkg^{-1} to LPI > 50 Jkg^{-1}), the probability of lightning discharge occurrence was ca 30–90% and the proportion of successfully predicted lightning discharges reached up to 77%. We consider this result satisfying, though the spatial verification remains challenging. Contrary to spatial verification of LPI, the temporal verification of LPI turned out to be even more efficient (in 70% of cases the time difference between the defined beginnings of forecasted and detected lightning activity was maximum 45 min). In future, we plan to perform lightning prediction in another NWP model, namely the ICON NWP model. We also plan to analyse more thunderstorm events.

1. Introduction

Lightning activity is considered a severe meteorological hazard that needs to be studied, monitored as well as predicted. Lightning is closely related to strong convection in the atmosphere, which is a very complex phenomenon that is difficult to model. Such modelling is especially complicated if electrical processes must be included because our knowledge in this area is still incomplete. Thus, the forecast of lightning activity is very limited at present (Dementyeva et al., 2015; Gharaylou et al., 2019; Lynn and Yair, 2010; Mejsnar et al., 2018; Rezacova and Sokol, 2003; Sokol and Minářová, 2020; Yair et al., 2010).

There are several approaches to predict lightning occurrence. At present, the majority of prediction methods is based on using a numerical weather prediction (NWP) model and various indices which are related to convective or electrical processes. These indices indirectly describe and quantify atmospheric processes related to lightning. For example, the convective indices such as CAPE (Convective Available Potential Energy; Williams and Renno, 1993), CPTP (Cloud Physics Thunder Parameter; Bright and Wandishin, 2005), CAPE*P (CAPE combined with precipitation; Romps et al., 2018) or the Whiting

* Corresponding author at: Institute of Atmospheric Physics of the Czech Academy of Sciences, Boční II 1401, 141 00 Prague, Czech Republic.
E-mail address: sokol@ufa.cas.cz (Z. Sokol).

https://doi.org/10.1016/j.atmosres.2022.106025
Received 30 March 2021; Received in revised form 4 January 2022; Accepted 7 January 2022
Available online 11 January 2022

coefficient (Sturtevant, 1995) are usually employed. Yair et al. (2010) introduced another useful lightning prediction tool, the Lightning Potential Index (LPI).

The LPI is defined as the kinetic energy of the updraft in a developing thundercloud scaled by the potential for charge separation based on mixing ratios of ice and liquid water within the main charging zone (from 0 °C to −20 °C) of the cloud (Yair et al., 2010). The LPI can have non-negative values that are given in Jkg^{-1}. Yair et al. (2010) and Lynn and Yair (2010) also suggested that the LPI is not only a useful parameter for lightning prediction, but also a helpful tool for improving weather forecasts of convective storms and heavy rainfall. Several studies (e.g. Gharaylou et al., 2019) confirm that the LPI has better performance in prediction of lightning occurrence than other indices. Wang et al. (2011) showed a good spatial and temporal consistence of calculated LPI with observed lightning flashes. Moreover, Ou Jianfang et al. (2019) suggested that the LPI can be used to forecast lightning density.

Sokol and Minářová (2020) found that the LPI is a promising tool in predicting the lightning activity in the region of the Czech Republic, Central Europe. In their study, they calculated the LPI within the COSMO NWP model (http://www.cosmo-model.org). This study builds on their study and uses the same model forecasts. The current study, however, aims at spatial and temporal analyses of LPI prognostic fields calculated for 10 thunderstorm events which occurred in 2018 in the Czech Republic. Contrary to Sokol and Minářová (2020), our study does not evaluate the potential of the use of LPI, though verifies the lightning prediction as such. In addition, this paper newly compares the distribution of model and observed lightning activity in dependence on orography and their spatial and temporal distributions. Thus, the main focus of this study is on spatial and temporal verification of the LPI fields using ground-based measurements of lightning discharges.

This paper is organized as follows. After this introductory section, Section 2 describes the study region, COSMO NWP model setup, verification methods, and observed data of lightning. Section 3 provides examples of predicted LPI, investigates different model setups, analyses LPI in relation to model orography, and presents and discusses the results of LPI verification in space and time. Section 4 is dedicated to a discussion of presented study in comparison with our previous study and finally Section 5 draws conclusions of this paper.

2. Data and methods

2.1. Study region

The region considered in this study (Fig. 1) matches with the model domain of the COSMO NWP model. The whole region is covered by a grid of 271 × 231 nodes with a horizontal step of 1.2 km. Fig. 1 also shows the model orography of the study region, which spans from 108 to 1297 m ASL. It should be noted that the model orography is smoothed due to finite resolution of the COSMO NWP model, therefore it differs from a detailed digital elevation model in the highest elevations. However, the model orography maintains the general orographic features such as mountain ridges well. Fig. 2 shows the relative distribution of 5-m intervals of elevation in the study region.

2.2. Configuration of COSMO NWP model

We base this study on the same simulations as in Sokol and Minářová (2020), however, we analyse them deeper and verify the predictions in space and time. The COSMO NWP model used for our simulations was a non-hydrostatic convection-permitting model (http://www.cosmo-model.org), version 5.04d. Initial and boundary conditions were calculated using forecasts of the COSMO D2 model (https://www.dwd.de/SharedDocs/downloads/DE/modelldokumentationen/nwv/cosmo_d2/cosmo_d2_dbbeschr_version_1_0_201805.html), which were kindly provided by the German Weather Service. Boundary conditions having a time resolution of 1 h were available, and in between, they were linearly interpolated in time (Sokol and Rezacova, 2006). We used model namelists intended for the use in Europe, which were available together with the model code COSMO and did not change the defined model parameters.

We run the model for 10 selected thunderstorm events (Table 1) twice, differing in comprised cloud microphysical scheme, 1- and 2-moment (1M and 2M, respectively) cloud microphysics. In the model,

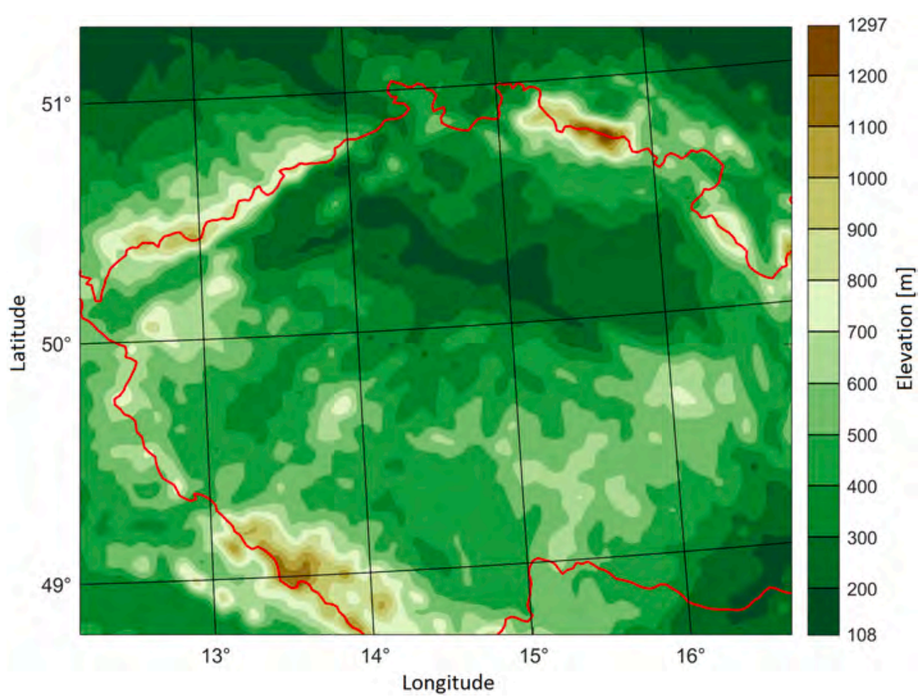

Fig. 1. Study area and the model orography. The red line indicates the borderline of the Czech Republic (Central Europe). (For interpretation of the references to colour in this figure legend, the reader is referred to the web version of this article.)

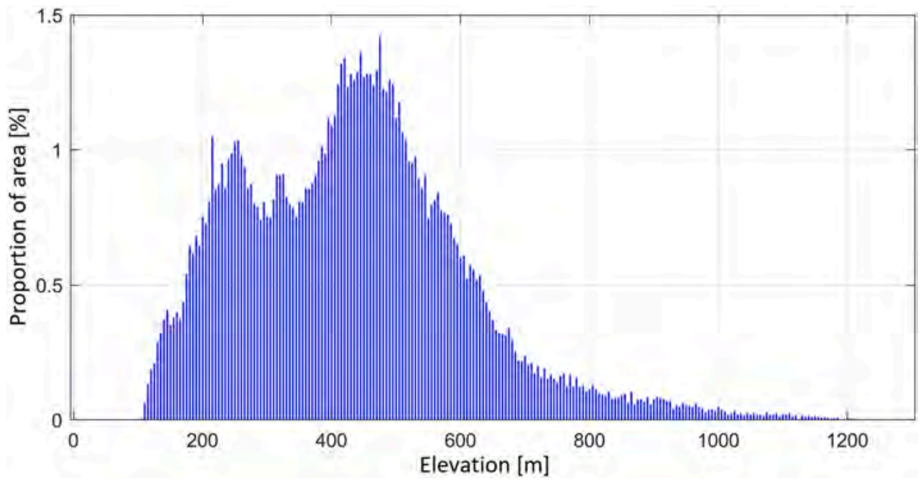

Fig. 2. The relative distribution of 5-m intervals of elevation (105–1300 m ASL) over the study area (Fig. 1).

Table 1
A list of examined events. First column gives the date of the event in the YYYYMMDD format, when a significant lightning activity occurred in the study region. Second column shows the beginning time in UTC of the simulation run in the COSMO NWP model. Third column denotes the total number of lightning discharges detected in the same region in the time frame of 12 h since the beginning of the forecast according to observations by EUCLID.

Event no.	Event [YYYYMMDD]	Beginning of the run [UTC]	No. of detected lightning discharges
1	20180601	06	47,580
2	20180610	06	28,378
3	20180705	12	2681
4	20180802	12	10,132
5	20180803	06	1070
6	20180804	12	12,309
7	20180808	12	15,114
8	20180813	12	1213
9	20180824	12	5278
10	20180921	12	5457

we computed LPI (option of the COSMO NWP model) prognostic values over the study region (Fig. 1) and used the values of LPI in the time step of 15 min.

Each simulation began at 06 or 12 UTC according to the time of the maximum intensity of individual thunderstorms and each model run provided a forecast with a lead time of up to 12 h. The time step of model integrations was 6 s, the vertical resolution covered 70 layers spanning from the model orography to 22 km. The model layers were unevenly distributed. Lower vertical layers were denser (i.e., their vertical resolution was higher, in the order of tens to first hundreds of m) than upper vertical layers for a more accurate physical description of the processes occurring near the ground.

2.3. *Verification data set – Detected lightning discharges*

For the 10 selected thunderstorm events (Table 1), we dispose of a dataset of ground-based observations of lightning flashes that we obtained for the Czech region from the German network Blitz Informationsdienst Siemens (BLIDS, new.siemens.com/global/de/produkte/services/blids.html), which is a part of the European Cooperation for Lightning Detection (EUCLID, https://www.euclid.org). BLIDS uses the time-of-arrival (TOA) principle based on detection of electromagnetic impulses induced by a lightning discharge. Each receiver registers the TOA of such individual impulse and by comparing the TOAs among receivers, location of the lightning discharge is found.

The data of detected lightning activity comprise following characteristics: exact time of occurrence of the discharge (with ms accuracy, in UTC), geographical coordinates of the discharge (in WGS84), type of the discharge, cloud-ground (CG) or cloud-cloud (CC), polarity of the discharge (positive "+" or negative "–"), peak current (in kA), and binary information on data quality. According to the binary information, the quality of all the obtained data was good. The median of spatial accuracy of the data at the confidence level of 95% was 600 m and the detection efficiency was almost 100% (Poelman et al., 2013).

When comparing the forecasted lightning activity with the detected one, it is important to know what kind of data we are dealing in this comparison with. Thus, it is important to carry out some basic characterization of the data of the recorded lightning discharges. In this study, we analysed spatiotemporal distribution of the data, diurnal course of the discharges and occurrence of the CG flashes related to model orography.

The spatiotemporal distribution analysis was in agreement with our expectation as well as other studies, for example with Novák and Kyznarová (2011) who studied lightning activity in the Czech Republic during the years 2002–2008. In our study, the general movement direction of events was found from the West to the East, which corresponds to the prevailing wind direction over the study region (Tolasz, 2007). Considering CG vs. CC types of discharges, the CC discharges were much more frequent, according to our expectations. On average, the CG flashes represented 19.9% of all recorded discharges, which agrees with theoretical assumptions (Rakov and Uman, 2007).

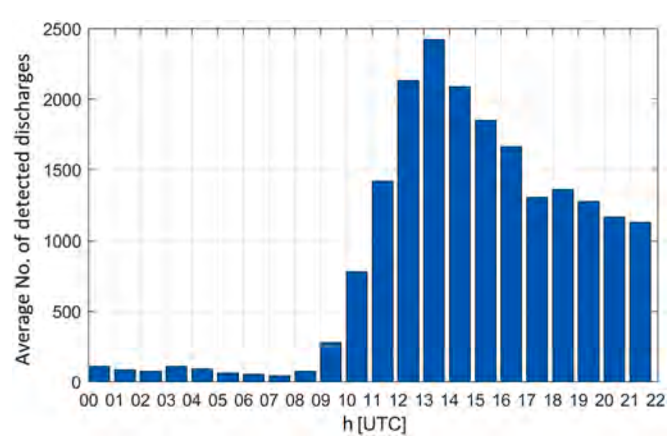

Fig. 3. The diurnal course of the number of detected lightning discharges per hour per event. The intervals 22-23 and 23-00 UTC are cut off due to a lack of data caused by a shift of the data from CEST (Central European Summer Time) to UTC.

Fig. 3 shows the diurnal course of the average number of detected lightning discharges with its clear peak in the early afternoon (13-14 UTC). The minimal lightning activity occurs late at night. The diurnal course corresponds well to other studies of this sort (e.g. Blakeslee et al., 2013; Enno et al., 2020).

The distribution of CG discharges related to the model orography of the study region is depicted in Fig. 4 (upper left). The distribution of CG flashes as such (not shown) corresponded quite well to the distribution of the 5-m intervals of elevation across the whole region (Fig. 2). The most of the lightning activity occurred between 200 and 600 m ASL since this interval represents 77.8% of the whole region. However, when related to a unit of area (1 grid square) it suggests that the lightning activity varies in its elevation-related frequency quite a lot (Fig. 4 upper left). The three remaining diagrams in Fig. 4 are discussed later in this paper.

In order to statistically test the relationship between elevation and distribution of CG discharges, we calculated both Pearson (R) and Spearman (R_S) correlation coefficients (Wilks, 2019). Usually, R is used to measure linear relationship, though according to general experience it can be used even if the theoretical assumptions on linearity are not met. However, it is clear (Fig. 4 upper left) that if there any correlation were, it would not be linear. We calculated R and R_S values for both sum of CG discharges and sum of CG discharges per 1 grid square (not shown and Fig. 4 upper left, respectively). In the first case, the R value was −0.63, whereas the R_S value was −0.69. For the second case (Fig. 4 upper left), the R value was −0.17, whereas the R_S value was −0.25. By testing all four values with a simple statistical *t*-test (with the confidence interval 95%) we got that the data cannot be regarded as independent. However, the obtained values are not significant enough to perform further analyses. The lack of a strong correlation between distribution of CG discharges and elevation can be explained by elevation not being the most dominant factor for formation of convection in the study region during considered events.

Other studies (e.g. Kotroni and Lagouvardos, 2008; Schulz and Diendorfer, 1999; Smorgonskiy et al., 2013) show general increase in lightning activity with elevation, though this tendency is very inconsistent throughout all considered terrain levels. They suggest that the dependence is complicated, which is in agreement with our findings.

2.4. Verification methods

Verification of the LPI prediction using the measured discharges is

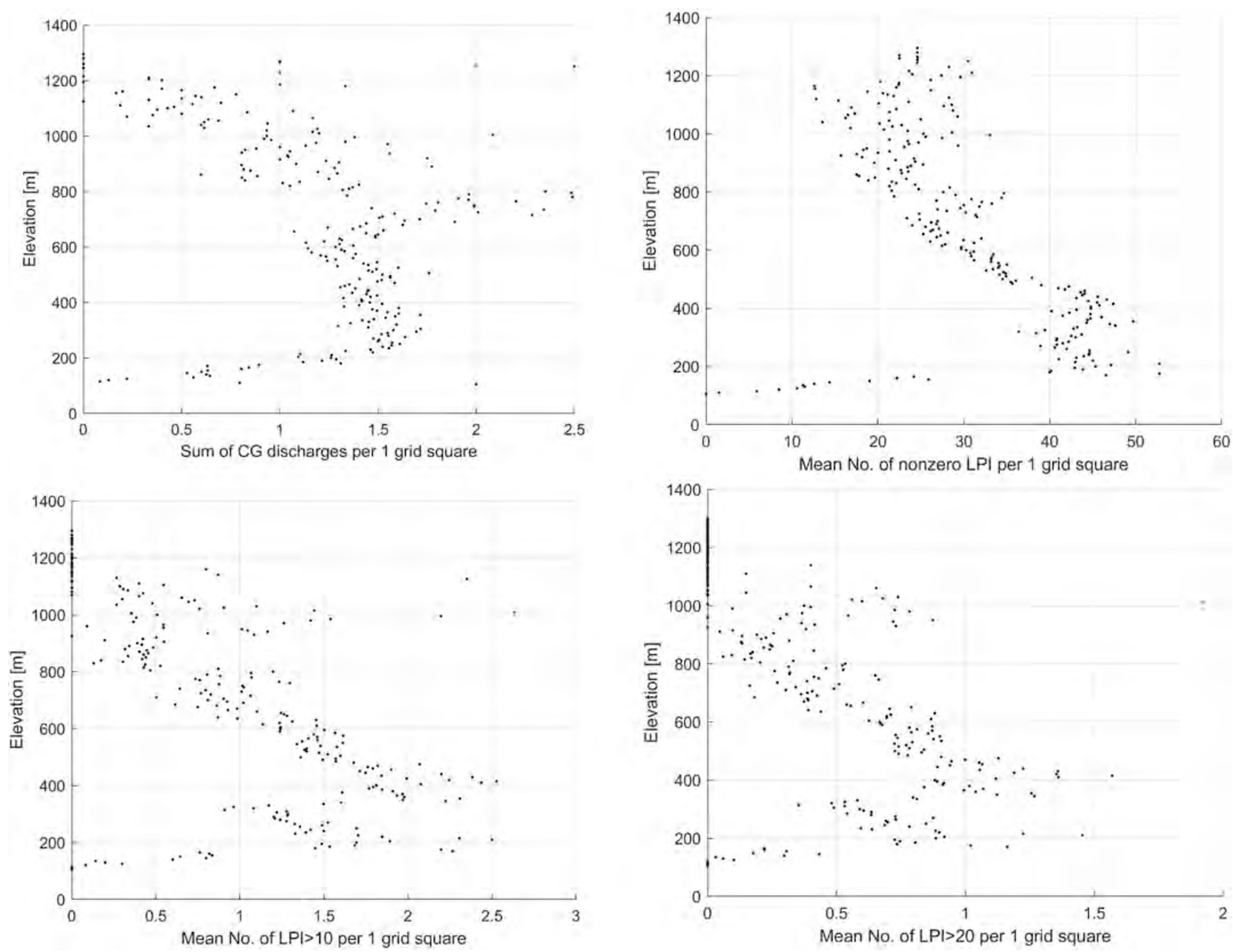

Fig. 4. The distribution of CG discharges and LPI prognostic values related to the model orography. Each point represents a 5-m interval of elevation (from 105 to 1300 m ASL). The upper left diagram depicts the weighted sums of CG discharges per 1 grid square, the weight being the ratio of the number of grid squares of the elevation interval to the number of grid squares of the whole region (Fig. 2). The upper diagram on the right and both bottom diagrams depict the distribution of the weighted number of LPI values corresponding to different thresholds (LPI > 0 Jkg^{-1}, LPI > 10 Jkg^{-1} and LPI > 20 Jkg^{-1}) per 1 grid square, the weight being the same as described above.

not straightforward, because the data of detected lightning activity is represented by a set of points specified by their absolute location in a geographical coordinate system, whereas the LPI prognostic values are given as planar information, which makes these two types of data not easy to compare with each other. Although the position of the measured discharges has a similar surface structure as the measured severe convective precipitation, the continuous character of LPI and discrete nature of the electrical data is not very suitable for the application of methods focused on verification of precipitation such as the Fraction Skill Score (FSS; Roberts and Lean, 2008) or similar techniques discussed by Wilkinson (2017). The problem consists in determining suitable thresholds of LPI values corresponding to selected thresholds of number of recorded lightning discharges in grid point area. Despite questionable use of FSS we carried out this analysis for both 1M and 2M cloud microphysics, its application and results are presented in Section 3.4. Moreover, we present the performance diagram combining four categorical skill scores for LPI forecasts using 1M and 2M cloud microphysics, although it is worth noting that verification methods based on point to point comparison are not very suitable due to discrete character of data leading to double error (miss and false alarm), e.g. Harvey et al. (1992). For the reason described above we also used another verification method, which estimates the forecast accuracy, and we denoted it pq-method. It is presented and discussed in detail in Section 3.4.

It is also important to bear in mind that the forecasted LPI values depend on the overall simulation in the NWP model. More precisely, location of predicted lightning occurrence depends on the location of simulated deep convection. Thus, the accuracy of lightning prediction in a given area is significantly influenced by the success of the model to forecast other weather features, which precede lightning. Therefore, the verification of the forecasts of lightning activity can be understood as the verification of the model ability to forecast strong convection and severe storms. Although the 2M cloud microphysics physically describes strong convection better than the 1M cloud microphysics (as discussed later in this paper), it is useful to know how this is reflected in quality of the lightning forecasts.

In this study, we examined the LPI prognostic fields in relation to detected lightning discharges both in space and in time, each individually. We verified the LPI prognostic values by the dataset of detected lightning discharges using two different approaches. In the first approach, we compared spatial distributions of the LPI values and detected lightning discharges by analysing the correlation between the LPI values and the proximity of recorded discharges and vice versa. In

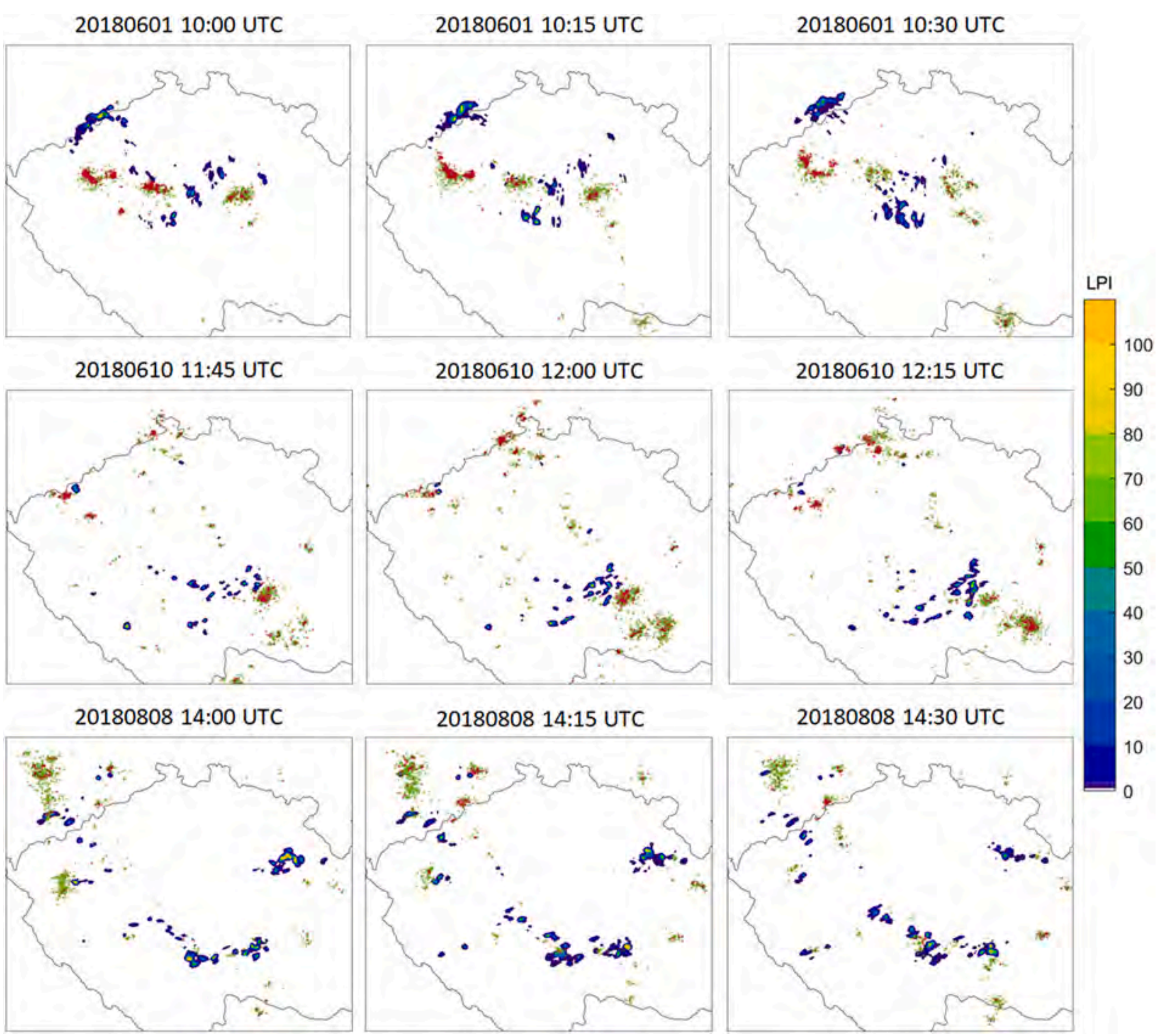

Fig. 5. An example of LPI prognostic values (colour scale) using 2M cloud microphysics depicted together with detected lightning discharges (CG red crosses, CC green crosses) for the three strongest thunderstorm events: 20180601 10:00–10:30 UTC, 20180610 11:45–12:15 UTC, and 20,180,808 14:00–14:30 UTC. Shown are the discharges detected in the time intervals 9:45–10:30, 11:30–12:15 and 13:45–14:30 UTC, respectively. Black line represents the borderline of the Czech Republic. (For interpretation of the references to colour in this figure legend, the reader is referred to the web version of this article.)

the second approach, we evaluated the concurrence of time courses of both forecasted and observed lightning activity, namely the sum of LPI values and the number of detected lightning discharges both across the whole study region (Fig. 1). For the verifications we only considered the LPI prognostic values given by the model simulation with the 2M cloud microphysics (the reason for that is discussed later in this paper).

3. Results and discussion

3.1. Examples of predicted LPI fields for three strongest thunderstorms

We defined three strongest thunderstorm events based on the highest total number of detected lightning discharges in the study region during given events. The three strongest thunderstorm events correspond to Events No. 1, 2 and 7 in Table 1. We selected these events to demonstrate the distribution of predicted and detected lightning activity. Fig. 5 shows examples of forecasted LPI fields (using 2M cloud microphysics) and compares them with observations of CG and CC flashes. All of the examples indicate a good spatial consistence of both types of data.

3.2. Comparison of 1M and 2M cloud microphysics

Before verification of the LPI prognostic fields as such, we compared the datasets of predicted lightning activity according to the 1M and 2M cloud microphysical schemes, similarly to Sokol and Minářová (2020) where histograms of the data were presented. However, in this study, we not only compared the LPI values given by 1M and 2M cloud microphysics, but also analysed them along with observed lightning activity.

We studied the overall frequencies of the LPI prognostic values calculated in the COSMO NWP model using 1M and 2M cloud microphysics. Table 2 gives an overview of basic characteristics of the LPI prognostic values, the values LPI $= 0$ Jkg^{-1} were excluded for the calculation of the mean LPI value (mean LPI) and for the calculation of the average frequency of LPI (mean N). As shown in Table 2, when considering the 2M cloud microphysics, the LPI prognostic values are not only higher, but also more frequent.

Moreover, we studied the relationship of detected and forecasted lightning activity along with 1M and 2M cloud microphysics. We carried out a linear regression of the sum of LPI values and the number of detected lightning discharges for four different combinations: 1M and 2M cloud microphysics each combined with either total lightning activity (CG + CC discharges) or CG discharges separately. This is a new analysis which was not performed in Sokol and Minářová (2020). For all four regression models, coefficients of determination (R^2, Wilks, 2019) were tested with a simple statistical *t*-test (with the level of significance 5%) and it was confirmed that the data cannot be regarded as independent. Both linear models considering 2M cloud microphysics proved to better fit the data than the models considering 1M cloud microphysics (Fig. 6, Table 3). This result is in agreement with the findings of Sokol and Minářová (2020), who showed by performing the Area under the Receiver Operating Characteristic (AROC) evaluation that using 2M cloud microphysics was more successful for lightning prediction by LPI.

Furthermore, we tried to distinguish CG activity from the total lightning activity to see if there were any significant difference.

Table 2
A summary of basic characteristics of the LPI prognostic values given by 1M and 2M cloud microphysics. Max LPI and mean LPI stand for the overall maximum value and the average value of LPI (excluding LPI $= 0$ Jkg^{-1}), respectively. Mean N is the average frequency of positive LPI values. Z_0 shows the proportion of occurrences of LPI $= 0$ Jkg^{-1}.

Cloud microphysics	max LPI [Jkg^{-1}]	mean LPI [Jkg^{-1}]	mean N	Z_0 [%]
1M	195.80	1.24	$2.28 * 10^3$	97.44
2M	460.52	1.66	$3.11 * 10^3$	96.51

However, we found out that the model fits slightly better when considering total lightning activity rather than CG discharges separately, thus for further analyses and verifications only total lightning activity is taken into account.

3.3. LPI characteristics related to model orography

Similarly to Section 2.3 (Fig. 4 upper left) where we showed the occurrence of CG discharges along with the model orography (namely sum of CG discharges per 1 grid square), we analysed the distribution of the LPI prognostic values in relation to the model orography as well (Fig. 4 upper right and both bottom diagrams). First of all, we investigated the overall distribution of grid points where LPI > 0 Jkg^{-1} (not shown). Then, we studied the distribution of LPI grid points depending on several different thresholds (examples for LPI > 0 Jkg^{-1}, LPI > 10 Jkg^{-1} and LPI > 20 Jkg^{-1} are shown in Fig. 4) which we used to calculate the number of grids in a unit of area (1 grid square).

The general distribution of LPI grid points in all of the cases (Fig. 4 upper right and both bottom diagrams) is consistent with the findings of detected lightning activity in Section 2.3 (Fig. 4 upper left). The overall predicted lightning activity (not shown) corresponded well to the model orography in study region (Fig. 2) as well as to the distribution of CG discharges (not shown). The distribution of LPI grid points per 1 grid square (the upper right diagram and both bottom diagrams in Fig. 4) preserves the general distribution compared to CG discharges per 1 grid square (Fig. 4 upper left), though the higher the LPI threshold, the less total number of LPI grid points and the less visible consistency of the distribution of the values. On the whole, the consistency of presented distribution of both predicted and observed lightning activity can be considered a good result indirectly confirming that the model microphysics is well applied in the COSMO NWP model.

Moreover, it is worth noting that in contrast to lightning activity (Fig. 4) a similar relationship between model elevation and accumulated precipitation forecast was not found (not shown). This agrees with analysis of convective precipitation performed by Sokol and Bližňák (2009). They used measured precipitation data to present that convective precipitation lasting up to 6 h does not depend on elevation in the study region.

3.4. Verification of the LPI prognostic values in space

As mentioned above, lightning prediction in NWP models depends on how well the model simulates the development of the atmospheric conditions and processes. Therefore, we verified the LPI prognostic values in space and in time, each individually. First, we performed the FSS analysis, then carried out the performance diagram and then used the pq-method to verify the LPI values in space.

3.4.1. The FSS

FSS values range from 0 (completely wrong forecast) to 1 (perfect forecast) and depend on size of squares (x) for which FSS is calculated. We considered x from 3 km up to 200 km. The FSS takes into account spatial information from the neighbourhood of a verified grid box. It does not give any information about quantitative accuracy, however, using FSS values one can determine the scale for which a given forecast is skilful and useful. The forecast is considered skilful for scale x if FSS (x) $\geq FSS_u = 0.5 + f_0/2$, where f_0 is the probability of occurrence of forecasted event (Roberts and Lean, 2008). In our case, the event is defined in such a way that at least a given number N_F of flashes is recorded in a given 15 min interval in a given grid point area. The frequency of flashes is very low, thus f_0 is approximately 0 and $FSS_u \approx 0.5$.

We calculated the dependence of FFS(x) for the following LPI threshold values T: 0.01, 10, 20, 30, 40, and 50 Jkg^{-1}. We tested several values of N_F, because N_F expresses the strength of the event. As expected, the results confirmed that the model is not able to forecast weak events, e.g. for $N_F = 1$. The FSS values for such events were always less than 0.5

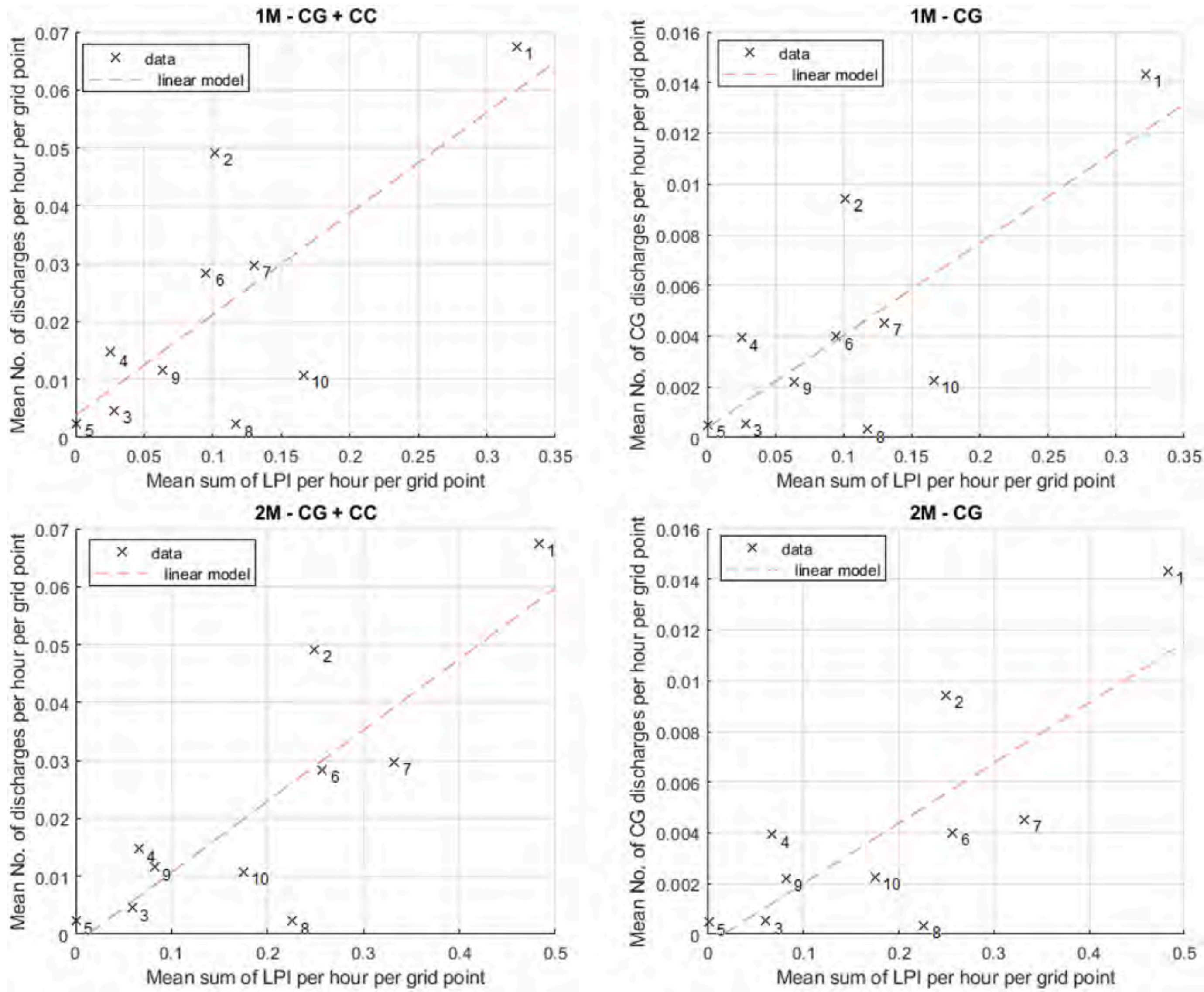

Fig. 6. A comparison of linear models for the sum of LPI values and the number of detected lightning discharges, both averaged per hour per grid square. Each symbol "x" represents one event (enumerated according to Table 1). Upper diagrams depict values according to the 1M cloud microphysics, lower ones according to the 2M cloud microphysics. Diagrams on the left show values for the total lightning activity, whereas diagrams on the right consider only CG discharges. Further information about these linear models is given in Table 3.

Table 3
A summary of basic characteristics of linear models depicted in Fig. 6. R^2 denotes the coefficient of determination of the particular linear model.

Cloud microphysics – type of lightning discharges	R^2	Linear model
1M – CG	0.56	$y = 3.7x * 10^{-2} + 3.8 * 10^{-4}$
2M – CG	0.61	$y = 2.4x * 10^{-2} - 3.8 * 10^{-4}$
1M – CG + CC	0.55	$y = 0.17x + 3.8 * 10^{-3}$
2M – CG + CC	0.69	$y = 0.12x - 1.6 * 10^{-3}$

for all considered x values. Fig. 7 presents FSS values dependent on x for $N_F = 5$ for both 1M and 2M cloud microphysics. In the case of 2M cloud microphysics, the forecast is skilful for scales around 90 km when we use LPI thresholds 30, 40 or 50 Jkg^{-1}. If we use the LPI threshold 20 Jkg^{-1}, the skilful scale is about 160 km. For 1M cloud microphysics skilful forecasts are reached at scales around 140 km for the LPI thresholds 30, 40 or 50 Jkg^{-1}, which is a larger scale in comparison to 2M cloud microphysics. However, the opposite is true for the LPI threshold 20 Jkg^{-1} where 1M cloud microphysics gives better results. We are not able to explain this result.

In our opinion, based on our experience with various values of N_F that we tested, $N_F = 5$ is a reasonable compromise between the intensity of the phenomenon and its predictability and thus we chose this value for the FSS analysis. The results obtained (Fig. 7) can be interpreted as follows. If the LPI $\geq$ 40 Jkg^{-1} in a grid point, then at least $N_F = 5$ discharges can be expected in the area of 90 $\times$ 90 km and 130 $\times$ 130 km around the grid point for the model with 2M and 1M cloud microphysics, respectively.

3.4.2. *The performance diagram*

Following the FSS analysis, we also used a combination of four well-known categorical skill scores derived from the 2 $\times$ 2 contingency table (Wilks, 2019): the probability of detection (POD), false alarm ratio (FAR), bias, and critical success index (CSI; also known as the threat score). These four skill scores are defined as follows:

$POD = a_{11}/(a_{10} + a_{01})$, (1)

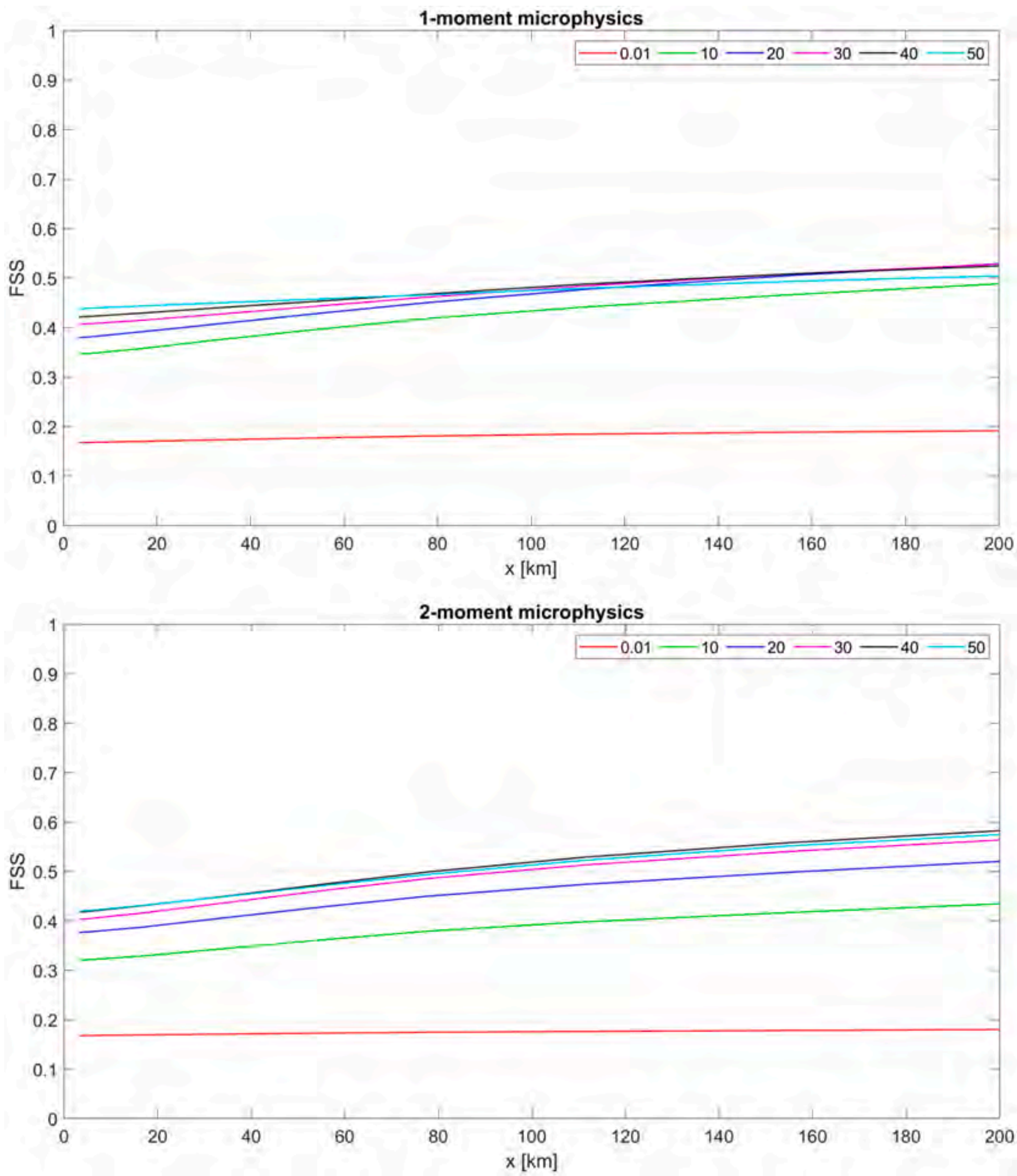

Fig. 7. The dependence of FSS values on scale x (3–200 km) for different LPI thresholds T (0.01, 10, 20, 30, 40, and 50 Jkg^{-1}) for 1M (upper diagram) and 2M (bottom diagram) cloud microphysics. The event is defined in such a way that at least $N_F = 5$ of flashes is recorded in a given 15 min interval in a given grid point area. Both N_F and LPI thresholds are related to the same areas and 15 min time intervals.

$FAR = a_{01}/(a_{11} + a_{10})$, (2)

$CSI = a_{11}/(a_{11} + a_{01} + a_{10})$, (3)

and

$bias = (a_{11} + a_{10})/(a_{11} + a_{01})$, (4)

where the a_{FO} coefficients in (1–4) are elements of the contingency table. The index O = 0/1 indicates the event observation (with O = 1 if the event was observed and O = 0 if it was not). The index F = 0/1 relates to event forecast (where F = 1 if the event was forecasted and F = 0 if it was not). The POD, FAR, CSI, and bias can be presented in one figure, commonly called the performance diagram (e.g. Rezacova et al., 2009; Roebber, 2009). Values of POD, 1-FAR, and CSI are between 0 (completely wrong) and 1 (perfect fit).

As mentioned earlier, application of skill scores may lead to double error. To partly reduce this problem, we covered the model area by smaller square areas with sides of 36, 60, 84, and 108 km and defined an event for mean values of these areas. These squares were arranged to cover the inside of the model area but not to overlap. The centre of the model area and the centre of each whole area consisting of smaller squares were the same. The edges of the model area remained uncovered. It should be noted that the results can be affected by the number of squares for which events are defined, since they significantly vary depending on their size.

We defined the events by a comparison of thresholds T_{LPI} and T_{OBS} with the average LPI per grid point in the single squares (M_{LPI}) and the average number of observed lightning strikes per grid point in the same squares (M_{OBS}). The event occurred if $T_{LPI} \geq M_{LPI}$ and similarly $T_{OBS} \geq M_{OBS}$. Note that T_{LPI} and T_{OBS} are different quantities. In order to find corresponding values, we compared the percentiles of all observed and forecasted grid point values. We chose the 90th, 95th, 97th, and 99th percentiles to define the thresholds, namely $T_{OBS} = 1, 9, 22, 81$ and $T_{LPI} = 1.105, 63.36, 217.07, 861.69$, respectively, for forecasts using 2M cloud microphysics. In the case of 1M cloud microphysics, T_{OBS} were the same and $T_{LPI} = 0.320, 33.395, 119.18, 502.615$, respectively. The chosen thresholds were the same for all square sizes and were intentionally selected quite high to see how successful the forecast of severe events is. This choice was based on the fact that prediction of severe storms is important mainly from the practical point of view.

Fig. 8 shows the values of POD, 1-FAR, CSI, and bias for the four thresholds T_{OBS} and corresponding T_{LPI}, and for four different sizes of squares: 36 × 36 km, 60 × 60 km, 84 × 84 km, and 108 × 108 km. Small square and cross symbols in Fig. 8 show results of forecasts of 2M and 1M cloud microphysics, respectively. Each symbol occurs four times corresponding to square sizes, namely the larger the square, the larger the CSI.

Fig. 8 indicates that forecasts using the 2M cloud microphysics give slightly higher CSI than 1M cloud microphysics. However, the hypothesis that 2M cloud microphysics provides significantly higher CSI than 1M cloud microphysics (for selected thresholds and sizes of squares) was rejected by a bootstrap test at probabilistic level of 90% almost for all forecasts. The bootstrap test used random samplings of the observed and the forecasted data with replacement from the sample data to estimate confidence intervals for parameters of interest. We applied the predefined function bootci (bootstrap confidence interval) in MATLAB software (www.mathworks.com).

Fig. 8 clearly demonstrates that higher values of CSI are obtained for larger areas and lower thresholds. This can be explained by that the effect of double error is reduced for the larger squares and that presumably the accuracy of prediction decreases with increasing extremity of the event. It is worth noting that for all presented types of forecasts, the bias is close to unity, which is a consequence of the fact that the thresholds were selected on the basis of the same percentiles for both observed and forecasted values.

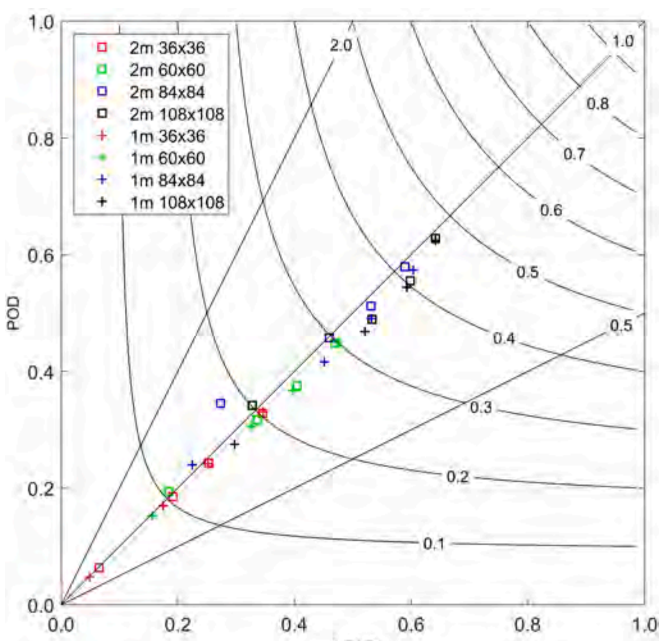

Fig. 8. The performance diagram combining POD, 1-FAR, CSI, and bias for $T_{OBS} = 1, 9, 22, 81$. Thresholds $T_{LPI} = 1.105, 63.36, 217.07, 861.69$ for 2M cloud microphysics and $T_{LPI} = 0.32, 33.395, 119.18, 502.615$ for 1M cloud microphysics. Shown are the values corresponding to four different sizes of squares: 36 × 36 km, 60 × 60 km, 84 × 84 km, and 108 × 108 km. Each item of the legend represents results for four square sizes mentioned above. The highest CSI values correspond to largest squares and with decreasing square size CSI also decreases. Small square and cross symbols represent the results of forecasts using 2M and 1M cloud microphysics, respectively. The curves indicate the values of CSI and the straight lines starting from point [0,0] stand for bias = 0.5, 1, and 2.

3.4.3. The pq-method

In order to verify the predicted lightning activity in space using the pq-method, we first analysed the distances between each grid point where LPI exceeded a given threshold (we tested different thresholds from LPI > 0 Jkg^{-1} to LPI > 50 Jkg^{-1}) and its nearest detected discharge that occurred within 15 min, these two making a pair. We investigated how many of these pairs (LPI grid point + nearest discharge) occurred within a certain distance and denoted the proportion of the pairs by p. We tested several distances from 15 to 90 km. Then, we calculated the average *p* value of each event and average value (denoted mean p) of all events for given threshold of LPI and distance limit, as presented in Table 4.

The mean p characteristic can be interpreted as the probability of occurrence of a lightning discharge within given distance from a grid point where LPI has a certain value. For instance, according to Table 4, the probability of having a lightning discharge within 30 km from a grid point where LPI > 20 Jkg^{-1} is almost 75%. It can be summarized that the greater distance limit and also the higher LPI threshold, the higher probability of occurrence of lightning discharges. These results provide answers to a question on what one can expect in the area surrounding a given grid point when LPI in the grid point is greater than a certain threshold.

However, this characteristic ignores those cases when lightning was observed but LPI was zero or below the given threshold (i.e. so-called misses). The characteristic also misses the information about the lightning activity that occurs in a greater distance than where predicted (including the maximum tested limit: 90 km). Thus, we also investigated the relationship between the LPI prognostic values and nearest detected discharges vice versa. We analysed whether there was a grid point with LPI > 0 Jkg^{-1} and how far it was to each detected discharge (these two making a pair again) within given distance limit (15–90 km), depending on the threshold of the LPI value (from LPI > 0 Jkg^{-1} to LPI > 50 Jkg^{-1}). In order to interpret this analysis, we calculated the proportion of the pairs to all detected discharges and denoted it by q. Similarly, as mentioned above, we focused on the mean q values given in Table 5.

In fact, the mean q characteristic gives information about the proportion of successfully predicted lightning discharges depending on distance and LPI threshold. For example, on average, 12.5% of all lightning discharges were predicted by LPI > 20 Jkg^{-1} within 30 km (Table 5). This characteristic answers the question on how successfully the model indicates observed lightning.

Based on this characteristic, it can be summarized that the lower LPI threshold and the greater distance limit, the higher proportion of successfully predicted lightning discharges. The decrease of mean q values along with increasing LPI can also be explained by the frequency of LPI values introduced in Section 3.2 where we showed that higher LPI values are generally less frequent. Nevertheless, it is important to mention that this analysis does not consider one of the errors in the double error problem, namely the mean q values are independent of the extent of LPI prognostic fields. For instance, for a 100% success it would be enough for a model to predict positive LPI values in the whole study region. This also is one of the reasons we investigated mean q for different thresholds of LPI. In this sense, the previous "p-method" is stricter than the "q-method".

Table 4
An overview of the mean *p* values for each tested LPI threshold and distance limit. LPI thresholds are given in Jkg^{-1}.

Distance limit	LPI > 0	LPI > 10	LPI > 20	LPI > 30	LPI > 40	LPI > 50
15 km	0.3019	0.4191	0.5043	0.5337	0.5717	0.5843
30 km	0.5068	0.6371	0.7485	0.7166	0.7393	0.7400
45 km	0.6276	0.7720	0.8408	0.8198	0.7996	0.7968
60 km	0.7057	0.8178	0.8719	0.8514	0.8339	0.8333
75 km	0.7697	0.8612	0.9053	0.8938	0.8830	0.8870
90 km	0.8147	0.8834	0.9269	0.9194	0.9151	0.9216

Table 5
An overview of the mean q values for each tested LPI threshold and distance limit. LPI thresholds are given in Jkg^{-1}.

Distance limit	LPI > 0	LPI > 10	LPI > 20	LPI > 30	LPI > 40	LPI > 50
15 km	0.2145	0.0707	0.0517	0.0410	0.0321	0.0269
30 km	0.3519	0.1559	0.1250	0.1016	0.0851	0.0703
45 km	0.4755	0.2466	0.1990	0.1762	0.1555	0.1384
60 km	0.5953	0.3357	0.2751	0.2414	0.2140	0.1889
75 km	0.6970	0.4245	0.3436	0.2997	0.2666	0.2272
90 km	0.7688	0.4808	0.4069	0.3518	0.3088	0.2665

It is worth mentioning that it was only in 4% of all cases (considering 15 min prediction intervals) where none of all detected lightning discharges were predicted within the maximum distance of 90 km. The values of both mean p and mean q showed that the lightning prediction and its successfulness varied depending on the distance limit and the LPI threshold. By a suitable choice of the distance limit and the LPI threshold, the accuracy of the forecast can be optimized according to one's requirements.

It is also important to note that in at least two cases out of the 10 simulated thunderstorms (event no. 5 and 8 in Table 1), the model incorrectly predicted the development of the meteorological situation and especially the development of convection in the verified area (Sokol and Minářová, 2020), which of course negatively affected the mean p and mean q values in Table 4 and Table 5, respectively. However, these cases of inaccurate predictions occur in practice, and therefore we did not exclude them from the data.

3.5. Verification of the LPI prognostic values in time

In order to verify the LPI prognostic values in time, we used a semi-subjective method since full objectivity was not possible due to inconsistency among the events. We assessed the concurrence of the time courses of the detected and forecasted lightning activity, independent of their spatial location in study domain. We compared the time difference in 15 min time intervals between forecasted (LPI values in the time step of 15 min) and detected (15 min summed number of observed discharges) beginning of the event both defined by a combination of a local maximum with a sudden increase (jump) in the values. Fig. 9 presents the selected beginnings by vertical dashed lines and Table 6 gives the resulting time difference between the beginnings.

In some cases in Fig. 9 and Table 6, the predicted lightning activity corresponds quite well with the detected one with a time difference between the beginnings 0 min (event no. 3 and 4 in Table 1). On the other hand, some of the events show a significant inconsistency in the temporal concurrence of the predicted and forecasted lightning activity. The worst result for the event no. 1 (Table 1) in Fig. 9 and Table 6 might be related to the fact that this event showed quite low values of FSS for a rain rate above 5 mm/h (Sokol and Minářová, 2020), which means that meteorologically, this event was not very well predicted by the model. The same applies to the two aforementioned events (no. 5 and 8 in Table 1) with a time difference between the beginnings +45 min and −60 min, respectively (Table 6), which were predicted incorrectly and even excluded by Sokol and Minářová (2020) for further analyses due to FSS values close to zero.

In general, in 50% of all cases, the time difference between the defined beginnings of forecasted and detected lightning activity was 15 min or less (Fig. 9, Table 6). It was 45 min or less in 70% of the cases and in 90% of all cases the time difference was 60 min or less. To have a temporal inaccuracy of only one hour can be considered a fair outcome.

4. Discussion related to the previous study

Even though our study is based on the same COSMO NWP model runs as in Sokol and Minářová (2020), the current analysis is much deeper and brings new knowledge. We analysed the simulations with 1M and 2M cloud microphysics in more details and we verified the LPI prognostic values in space and time. Specifically, we constructed linear models for the sum of LPI values and the number of detected lightning discharges both averaged per hour per grid square as a function of LPI. Their accuracy expressed by R^2 convincingly shows that using 2M cloud microphysics gives better results than 1M cloud microphysics, thereby provides a clear evidence to the suggestion made by Sokol and Minářová (2020).

In this study, we newly compared and found reasonable agreement between relationships of the predicted lightning activity expressed by LPI and the model orography and observed lightning activity and the model orography. This agreement supports the statement that the model microphysics is well applied in the COSMO NWP model and the LPI has a good physical background.

Contrary to the previous study (Sokol and Minářová, 2020), where the Receiver Operating Characteristics was used, which evaluates the potential of the method, we compared the predicted LPI directly with observations in time and space. For the spatial verification, we considered distances from grid points with positive LPI to recorded lightning discharges and vice versa, and for the temporal verification, we analysed the time differences between predicted and detected beginnings of each lightning event. The verification methods used in this study are more illustrative, especially in terms of practical application of the method. Verifications of the results confirm that LPI is a useful forecasting tool for lightning prediction.

5. Conclusion

In this study, which is a continuation of our previous work (Sokol and Minářová, 2020), we investigated 15 min prognostic values of LPI calculated by the COSMO NWP model for 10 thunderstorm events which occurred in 2018 in Central Europe. We verified them in space and time against detected lightning activity using new methods. We also analysed both predicted and recorded lightning activity in relation to the model orography, which according to the best of our knowledge was performed for the first time in the case of forecast. Moreover, we compared different model runs using 1M and 2M cloud microphysics, newly in relation to the recorded lightning activity.

Our conclusions can be summarized as follows:

- 2M cloud microphysical scheme is more suitable for lightning forecasts based on LPI than 1M cloud microphysical scheme.
- Distribution of LPI values related to model orography corresponds well with that of recorded CG discharges, which confirms a good physical background of both the COSMO NWP model microphysics and the LPI.
- The FSS revealed that for 2M cloud microphysics we mostly reached a skilful forecast at smaller scales than for 1M microphysics, namely at scales around 90 km if we used LPI thresholds 30, 40, and 50 Jkg^{-1}.
- The performance diagram presented that higher values of CSI are obtained for larger areas and lower thresholds. In contrast to the other results, this evaluation did not confirm that forecasts using 2M cloud microphysical scheme were more accurate than forecasts using 1M cloud microphysical scheme.
- Spatial verification of LPI (the pq-method) showed that depending on the distance limit (15–90 km) and the LPI threshold (from LPI > 0 Jkg^{-1} to LPI > 50 Jkg^{-1}), the probability of lightning discharge occurrence was ca 30–90% and the proportion of successfully predicted lightning discharges varied from 3 to 77%. The low success results when inappropriate parameters (LPI threshold in particular) are selected. Thus, based on our results one can select a suitable distance limit and LPI threshold which optimise the forecast accuracy.

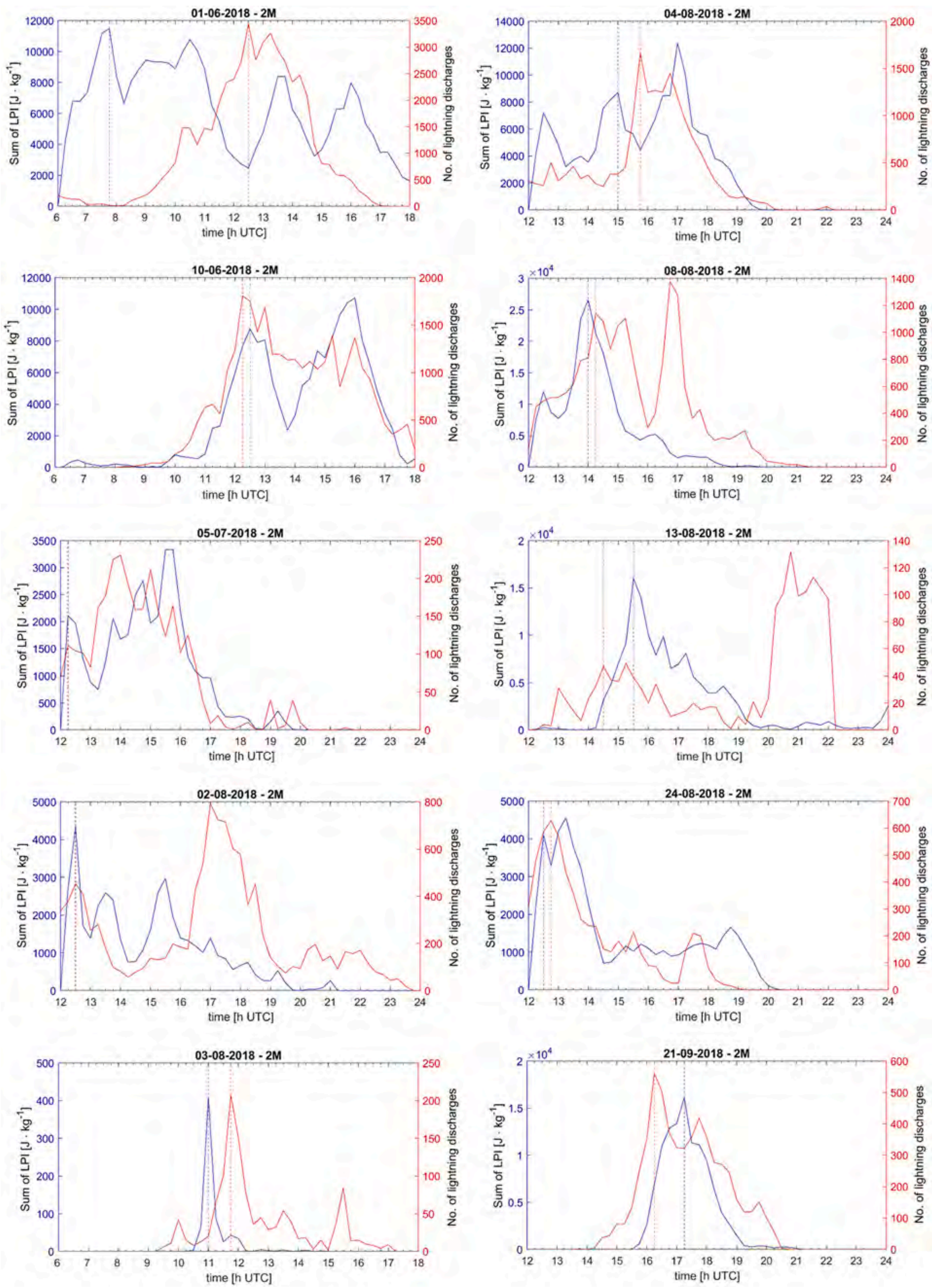

Fig. 9. An overview of analysed time courses of both the sum of the LPI prognostic values (blue) and the number of detected lightning discharges (red) over corresponding 12-h-long intervals. The vertical dashed lines indicate the beginning of each event. Caption above each diagram gives the date of the depicted event, 2M stands for the 2M cloud microphysics used in the simulations. (For interpretation of the references to colour in this figure legend, the reader is referred to the web version of this article.)

Table 6
An overview of the time differences between the predicted and observed beginnings of each studied event. Negative (positive) values denote the events in which the detected beginning occurred earlier (later) than the forecasted one.

Event	Time difference
20180601	285 min
20180610	−15 min
20180705	0 min
20180802	0 min
20180803	45 min
20180804	45 min
20180808	15 min
20180813	−60 min
20180824	15 min
20180921	−60 min

- In only 4% of all cases (considering 15 min prediction intervals) none of all detected lightning discharges were predicted by LPI within the maximum tested distance of 90 km.
- Temporal verification of LPI (considering time courses of predicted and detected lightning activity, omitting their spatial location) was semi-subjective though successful. In 50% of all cases the time difference between the defined beginnings of forecasted and detected lightning activity was up to 15 min, it was up to 45 min in 70% of all cases and up to 60 min in 90% of all cases.
- The temporal approach to verification of LPI offers higher potential to use than the spatial approach, which is in good agreement with conclusions of Ou Jianfang et al. (2019).
- In our opinion, the obtained results confirm that the LPI is a suitable tool for operative prediction of lightning. At the same time, our conclusions support the introduction of 2-moment cloud microphysics into the numerical weather forecasts.

Further work should be dedicated to lightning prediction using other NWP models, such as the ICON NWP model. In addition, it would be worth analysing more recorded thunderstorm events. It would also be interesting to compare predicted lightning activity with other types of meteorological data (e.g. precipitation, hail, wind gusts). Last but not least, it is worth performing assimilation of observed lightning data into NWP model, which may improve the spatial and/or temporal aspects of LPI forecasts.

Declaration of Competing Interest

The authors declare that they have no known competing financial interests or personal relationships that could have appeared to influence the work reported in this paper.

Acknowledgement

The research was funded by the project CRREAT (reg. number: CZ.02.1.01/0.0/0.0/15_003/0000481), call number 02_15_003 of the Operational Programme Research, Development, and Education, by the Technology Agency of the Czech Republic (grant no. SS02030040, PERUN), by project Strategy AV21, Water for Life, and by Charles University (UNCE/HUM 018). The authors very much appreciate the comments of the anonymous reviewers, which significantly helped to improve the manuscript. Many thanks also belong to BLIDS for providing lightning data.

References

Blakeslee, R., Mach, D., Bateman, M., Bailey, J., 2013. Seasonal variations in the lightning diurnal cycle global electric circuit. Atmos. Res. 135–136. https://doi.org/10.1016/j.atmosres.2012.09.023.

Bright, D.R., Wandishin, M.S., 2005. A physically based parameter for lightning prediction and its calibration in ensemble forecasts. In: Preprints, Conf. on Meteor. Applications of Lightning Data. Presented at the Conference on Meteorological Applications of Lightning Data, San Diego, California, USA.

Dementyeva, S., Il'in, N., Mareev, E., 2015. Calculation of the Lightning Potential Index and Electric Field in Numerical Weather Prediction Models. Известия Российской академии наук. Физика атмосферы и океана, 51, pp. 210–217. https://doi.org/10.7868/S0002351515010022.

Enno, S.-E., Sugier, J., Alber, R., Seltzer, M., 2020. Lightning flash density in Europe based on 10 years of ATDnet data. Atmos. Res. 235, 104769 https://doi.org/10.1016/j.atmosres.2019.104769.

Gharaylou, M., Farahani, M.M., Hosseini, M., Mahmoudian, A., 2019. Numerical study of performance of two lightning prediction methods based on: Lightning Potential Index (LPI) and electric POTential difference (POT) over Tehran area. J. Atmos. Sol. Terr. Phys. 193, 105067 https://doi.org/10.1016/j.jastp.2019.105067.

Harvey, L.O., Hammond, K.R., Lusk, C.M., Mross, E.F., 1992. The application of signal detection theory to weather forecasting behavior. Mon. Weather Rev. 120, 863–883. https://doi.org/10.1175/1520-0493(1992)120<0863:TAOSDT>2.0.CO;2.

Jianfang, O., Haixia, Q., Haitao, W., 2019. Establishment and test of a Lightning Potential Prediction Index. Meteorol. Environ. Res. 10, 51–54. https://doi.org/10.19547/j.issn2152-3940.2019.05.011.

Kotroni, V., Lagouvardos, K., 2008. Lightning occurrence in relation with elevation, terrain slope, and vegetation cover in the Mediterranean. J. Geophys. Res. 113. https://doi.org/10.1029/2008JD010605.

Lynn, B., Yair, Y., 2010. Prediction of lightning flash density with the WRF model. Adv. Geosci. 23, 11–16. https://doi.org/10.5194/adgeo-23-11-2010.

Mejsnar, J., Sokol, Z., Minářová, J., 2018. Limits of precipitation nowcasting by extrapolation of radar reflectivity for warm season in Central Europe. Atmos. Res. 213. https://doi.org/10.1016/j.atmosres.2018.06.005.

Novák, P., Kyznarová, H., 2011. Climatology of lightning in the Czech Republic. Atmos. Res. 100, 318–333. https://doi.org/10.1016/j.atmosres.2010.08.022.

Poelman, D.R., Schulz, W., Vergeiner, C., 2013. Performance characteristics of distinct lightning detection networks covering Belgium. J. Atmos. Ocean. Technol. 942–951. https://doi.org/10.1175/JTECH-D-12-00162.1.

Rakov, V.A., Uman, M.A., 2007. Lightning: Physics and Effects. Cambridge University Press.

Rezacova, D., Sokol, Z., 2003. A diagnostic study of a summer convective precipitation event in the Czech Republic using a nonhydrostatic NWP model. Atmos. Res. 67–8, 559–572. https://doi.org/10.1016/S0169-8095(03)00073-5.

Rezacova, D., Zacharov, P., Sokol, Z., 2009. Uncertainty in the area-related QPF for heavy convective precipitation. Atmos. Res. 93, 238–246. https://doi.org/10.1016/j.atmosres.2008.12.005.

Roberts, N.M., Lean, H.W., 2008. Scale-selective verification of rainfall accumulations from high-resolution forecasts of convective events. Mon. Weather Rev. 136, 78–97. https://doi.org/10.1175/2007MWR2123.1.

Roebber, P.J., 2009. Visualizing multiple measures of forecast quality. Weather Forecast. 24, 601–608. https://doi.org/10.1175/2008WAF2222159.1.

Romps, D.M., Charn, A.B., Holzworth, R.H., Lawrence, W.E., Molinari, J., Vollaro, D., 2018. CAPE times P explains lightning over land but not the land-ocean contrast. Geophys. Res. Lett. 45, 12,623–12,630. https://doi.org/10.1029/2018GL080267.

Schulz, W., Diendorfer, G., 1999. Lightning characteristics as a function of altitude evaluated from lightning location network data. In: Presented at the International Conference on Lightning and Static Electricity. https://doi.org/10.4271/1999-01-2310, pp. 1999-01–2310.

Smorgonskiy, A., Rachidi, F., Rubinstein, M., Diendorfer, G., 2013. On the relation between lightning flash density and terrain elevation. In: Presented at the 2013 International Symposium on Lightning Protection, SIPDA 2013, pp. 62–66. https://doi.org/10.1109/SIPDA.2013.6729216.

Sokol, Z., Bližňák, V., 2009. Areal distribution and precipitation–altitude relationship of heavy short-term precipitation in the Czech Republic in the warm part of the year. Atmos. Res. 94, 652–662. https://doi.org/10.1016/j.atmosres.2009.03.001.

Sokol, Z., Minářová, J., 2020. Impact of 1- and 2-moment cloud microphysics and horizontal resolution on Lightning Potential Index within COSMO NWP model. Atmos. Res. 237, 104862 https://doi.org/10.1016/j.atmosres.2020.104862.

Sokol, Z., Rezacova, D., 2006. Assimilation of radar reflectivity into the LM COSMO model with a high horizontal resolution. Meteorol. Appl. 13, 317–330. https://doi.org/10.1017/S1350482706002349.

Sturtevant, J.S., 1995. Základní nápověda pro předpovědi silných místních bouří. Florence, Ala.

Tolasz, R., 2007. Climate Atlas of Czechia. Czech Hydrometeorological Institute, Prague.

Wang, Y., Wan, Q., Meng, W., Liao, F., Tan, H., Zhang, R., 2011. Long-term impacts of aerosols on precipitation and lightning over the Pearl River Delta megacity area in China. Atmos. Chem. Phys. 11, 12421–12436. https://doi.org/10.5194/acp-11-12421-2011.

Wilkinson, J.M., 2017. A technique for verification of convection-permitting NWP model deterministic forecasts of lightning activity. Weather Forecast. 32, 97–115. https://doi.org/10.1175/WAF-D-16-0106.1.

Wilks, D.S., 2019. Statistical Methods in the Atmospheric Sciences. Elsevier Science.

Williams, E., Renno, N., 1993. An analysis of the conditional instability of the tropical atmosphere. Mon. Weather Rev. 121, 21–36. https://doi.org/10.1175/1520-0493(1993)121<0021:AAOTCI>2.0.CO;2.

Yair, Y., Lynn, B., Price, C., Kotroni, V., Lagouvardos, K., Morin, E., Mugnai, A., Llasat, M. del C., 2010. Predicting the potential for lightning activity in Mediterranean storms based on the Weather Research and Forecasting (WRF) model dynamic and microphysical fields. J. Geophys. Res. Atmosph. 115. https://doi.org/10.1029/2008JD010868.